$g_\perp$ signal. The data are consistent with a square-pyramidal geometry about Ir(II) with two trans PPh_3 ligands in the square basal plane and the third PPh_3 ligand in the apical position as shown in Scheme I. The unpaired electron then resides in the d_{z^2} orbital. Magnetic susceptibility measurements by the Gouy method on a solid sample of **2** at 26 °C gave a magnetic moment μ of 1.91 μ_B. Stable monomeric iridium(II) complexes are rare,[27,28] and most complexes of the d^7 Ir(II) ion known are dimeric with metal–metal bonds or metal–ligand–ligand–metal interaction. Electron spin resonance studies of $[IrBr_3(NO)(PPh_3)_2]$ and $[Ir(AsPh_3)(CNC_6H_4Me\text{-}p)(O_2CR)_2]$ indicate significant delocalization of the unpaired electron on the ligands.[27,28] The ESR spectrum shown in Figure 4, the first report of the spectrum of a monomeric cationic five-coordinate Ir(II) complex, likewise indicates considerable delocalization of the unpaired electron on the metal and the PPh_3 ligands.

It is noteworthy that the zerovalent radical complexes $[Rh(PPh_3)_2(CO)]$ and $[Ir(PPh_3)_2(CO)]$ rapidly scavenge chlorine from chlorocarbon solvents, but the iridium(II) radical **2** reacts more slowly with chlorocarbon solvents. The apparent stability of **2** must be attributed to resistance to dimerization by Coulombic repulsions of the cationic monomers, as well as the steric bulk of the three PPh_3 ligands, and the delocalization of the electron on the ligands.

The Ir–NO bond cleavage reaction, which was shown to proceed in the dark, is also enhanced by UV light. Since the reaction is enhanced by higher concentrations of PPh_3, the formation of the 18-electron complex $[Ir(NO)(CO)Cl(PPh_3)_3]^+$ (**3**) is expected. (See Scheme I where L is PPh_3.) Evidence for the formation of **3** was also indicated by the ^{31}P NMR data. Expulsion of NO from **3** as detected by IR and ESR spectra gives the paramagnetic compound $[Ir(CO)Cl(PPh_3)_3]^+$ (**2**). The iridium(II) compound **2** was found to decompose to form the Ir(I) and Ir(III) compounds *trans*-$[Ir(CO)Cl(PPh_3)_2]$ (**4**) and $[Ir(CO)Cl_3(PPh_3)_2]$. The formation of **4** was enhanced by UV irradiation.

The cleavage of the Ir–NO bond instead of the Ir–CO bond of $[Ir(NO)(CO)Cl(PPh_3)_2]^+$ in its thermal reaction with PPh_3 may be attributed to the weak Ir–NO bond in this compound. X-ray diffraction studies established that this compound has a structure with a weak bent $Ir{-}N{=}O$ bond[21] instead of a strong linear $Ir{=}N{=}O$ bond as has been reported for $[Ir(NO)(CO)(PPh_3)_2]$.[29] Molecular orbital considerations of the geometric and electronic structures of complexes with linear $M{=}N{=}O$ and with bent $M{-}N{=}O$ bonds have been presented, and the correlation diagram that should be applicable for the $[M(NO)(CO)(PPh_3)_2]$ complexes should be the diagram for the $\{MNO\}^{10}$ unit.[25] Since we have demonstrated the heterolytic cleavage of the Ir–N bond in the reaction of PPh_3 with compound **1**, which has a bent $Ir{-}N{=}O$ bond, and since the thermal reaction of $[Rh(NO)(CO)(PPh_3)_2]$ with PPh_3 proceeds with displacement of CO instead of NO from the strong linear $Rh{=}N{=}O$ bond, it is reasonable to propose that the cleavage of the Rh–NO bond in the photolysis of $[Rh(NO)(CO)(PPh_3)_2]$ proceeds by photoexcitation from a ground-state structure that has a strong linear $M{=}N{=}O$ bond to an excited state that has a weaker bent $M{-}N{=}O$ bond. The rhodium to nitrosyl ligand charge-transfer excited state is expected to be lowest in energy as d–d transitions are spin-forbidden for the d^{10} complex, and the Rh to ligand CO and PPh_3 charge-transfer transitions are expected to be at much higher energies. Zink and co-workers were the first to propose the photochemical consequence of a linear to bent geometry change in the photolysis of metal nitrosyl complexes.[5,30] Yang and Zink also determined the change from linear to bent geometry and the change in oxidation state for $K_2[Fe(CN)_5(NO)]$ by excited-state Raman spectroscopic studies.[31]

Acknowledgment. We thank the donors of the Petroleum Research Fund, administered by the American Chemical Society, for partial support of this research. This work was also supported by the National Science Foundation (Grant No. CHE-8410454). We thank the Perkin-Elmer Corp. for providing the Model 983 infrared spectrophotometer and the National Science Foundation (Grant No. CHE-8419266 and CH-855 1250) for partial funding for the IBM AF-200 FT NMR spectrometer. We thank Stephan Witt for recording the ESR spectra at the California Institute of Technology.

---

(27) Angoletta, M.; Beringhelli, T.; Morazzoni, F. *Spectrochim. Acta, Part A* **1982**, *38A*, 1177.

(28) Araneo, A.; Morazzoni, F.; Napoletano, T. *J. Chem. Soc., Dalton Trans.* **1975**, 2039.

(29) Brock, C. P.; Ibers, J. A. *Inorg. Chem.* **1972**, *11*, 2812.

(30) Liu, P.-H.; Zink, J. I. *Inorg. Chem.* **1977**, *16*, 3165.

(31) Yang, Y. Y.; Zink, J. I. *J. Am. Chem. Soc.* **1985**, *107*, 4799.

Contribution from the Department of Chemistry,
Southwest Missouri State University, Springfield, Missouri 65804

fac-*mer* Equilibrium in Solutions of VCl_3 in Acetonitrile[1]

J. F. O'Brien

Received August 8, 1986

Both the equivalent conductivity and the proton NMR spectra of solutions of vanadium trichloride in acetonitrile indicate the presence of a second species above 50 °C. The maximum value found for the equivalent conductivity, 6.21 $cm^2\ mol^{-1}\ \Omega^{-1}$ at 76 °C, is too low for a 1:1 electrolyte. The two species present are very likely the *fac* and *mer* isomers of $VCl_3{\cdot}3CH_3CN$.

Introduction

Early work[2-4] on the complexes of $TiCl_3$ and VCl_3 with nitriles suggested the presence in solution of only the neutral $MCl_3{\cdot}3CH_3CN$. Comparison of solution absorption spectra with diffuse reflectance spectra of the solids indicated that for both $TiCl_3$ and VCl_3 the species in solution were the same as the isolated solids. Confirmation of this was found in the low values of the equivalent conductivity.[3-5] The infrared spectra have been used in an attempt to distinguish between the *fac* and *mer* isomers.[4,6]

However, NMR line width data for the $TiCl_3$–CH_3CN system show two species present in the temperature range −40 to +80 °C.[7] One possibility is the *fac–mer* isomer pair. Another is $TiCl_3{\cdot}3CH_3CN$ and $TiCl_2{\cdot}4CH_3CN^+$. The similarity in spectral and electrical behavior between $TiCl_3$ and VCl_3 suggested that the NMR spectrum of VCl_3 would show a second species at higher

---

(1) Support of a grant from the Southwest Missouri State University Faculty Research Fund is gratefully acknowledged.

(2) Clark, R. J. H.; Lewis, J.; Machin, D. J.; Nyholm, R. S. *J. Chem. Soc.* **1963**, 379.

(3) McDonald, G. D.; Thompson, M.; Larsen, E. A. *Inorg. Chem.* **1968** 7, 648.

(4) Duckworth, M. W.; Fowles, G. W. A.; Hoodless, R. A. *J. Chem. Soc.* **1963**, 5665.

(5) Fowles, G. W. A.; Hoodless, R. A.; Walton, R. A. *J. Chem. Soc.* **1963**, 5873.

(6) Clark, R. J. H. *Spectrochim. Acta* **1965**, *21*, 955.

(7) O'Brien, J. F.; Eastman, M. P.; Alei, M., Jr. *Inorg. Chem.* **1970**, *9*, 1000.

0020-1669/87/1326-3264$01.50/0 © 1987 American Chemical Society

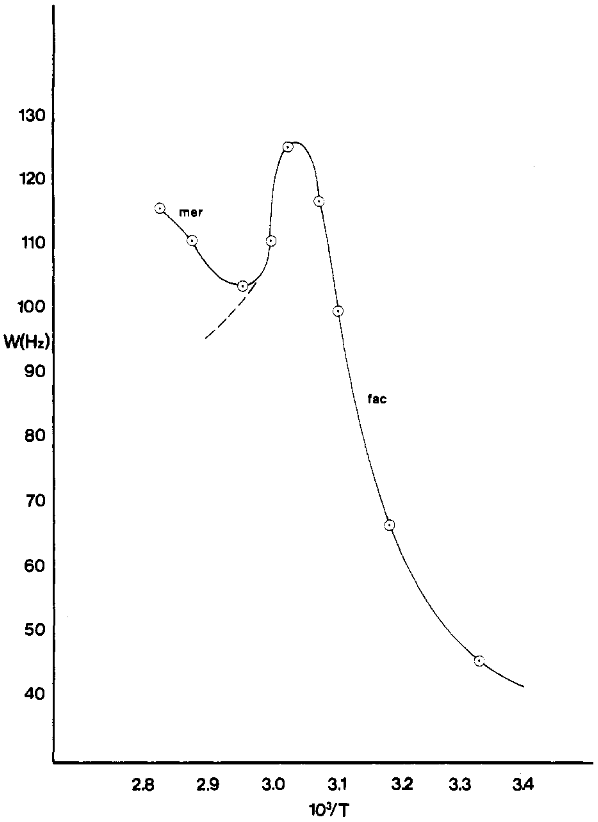

Figure 1. Proton NMR line width of 0.129 M VCl_3 in CH_3CN as a function of temperature.

temperatures. The equivalent conductivity at these higher temperatures would then permit assignment to either the *fac–mer* pair or the dissociation to $MCl_2^+ \cdot 4CH_3CN$.

The temperature dependence of the equivalent conductivity[8] in aqueous solutions obeys eq 1 with $x = 0.02$ for most ions.

$$\Lambda_{T_2} = \Lambda_{T_1}[1 + x(T_2 - T_1)] \qquad (1)$$

A similar relationship should hold in CH_3CN. Evaluation of x for a known strong electrolyte would then permit perdiction of values at temperatures above 25 °C. Comparison of calculated and measured values will then enable one to decide if an ionic species is present.

Experimental Section

CH_3CN was purified by distillation from P_2O_5 until its specific conductivity matched the literature value[2] of $(1-6) \times 10^{-7}\ \Omega^{-1}\ cm^{-1}$. VCl_3 was obtained from Alfa Products and used without further purification. The infrared spectrum of the VCl_3 in Nujol was recorded between 1500 and 250 cm^{-1} on a Perkin-Elmer 283 spectrophotometer using KRS-5 windows. The spectrum showed no evidence of V(IV) species. There were no peaks in the vanadium–oxygen region, 950–1050 cm^{-1}.[9] Tetraethylammonium bromide was obtained from Eastman Kodak and used without further purification. All solutions were prepared in glovebags under argon atmospheres. The conductivities were measured on a Beckman RC16B2 conductivity bridge. The cell constant of the Freas type cell was determined by using a 0.02 M aqueous solution of KCl at 25.0 °C. The NMR spectra were obtained on a Varian HA-60 spectrometer.

Results

The NMR line width as a function of temperature for a 0.129 M solution of VCl_3 in CH_3CN is given in Table I and shown in Figure 1.

The appearance of the curve requires the presence of a second species at the higher temperatures. If only one exchanging species was present, the data would follow the dotted line in the figure.

Table I. Line Width of Bulk Solvent Peak for 0.129 M VCl_3 in CH_3CN

T, °C	width, Hz	T, °C	width, Hz
28	45.5	62	110.2
42	60.6	66	103.2
49	99.2	75	110.4
54	116.5	81	115.5
59	125.3		

Table II. Equivalent Conductivity of 1.048×10^{-3} M Et_4NBr in CH_3CN as a Function of Temperature

10^4L	T, °C	Λ, $cm^2\ \Omega^{-1}$	10^4L	T, °C	Λ, $cm^2\ \Omega^{-1}$
4.79	15.0	164.5	6.08	45.0	208.0
5.19	25.0	178.5	6.38	55.0	219.5
5.67	35.0	194.5	6.86	65.0	235.5

Table III. Equivalent Conductivity of 0.0107 M VCl_3 in CH_3CN as a Function of Temperature

T, °C	Λ, $cm^2\ mol^{-1}\ \Omega^{-1}$	Λ(calcd), $cm^2\ mol^{-1}\ \Omega^{-1}$	T, °C	Λ, $cm^2\ mol^{-1}\ \Omega^{-1}$	Λ(calcd), $cm^2\ mol^{-1}\ \Omega^{-1}$
25	3.46	3.46	57	4.81	4.40
35	3.77	3.75	62	5.17	4.54
45	4.10	4.04	67	5.57	4.69
51	4.44	4.22	76	6.21	4.95

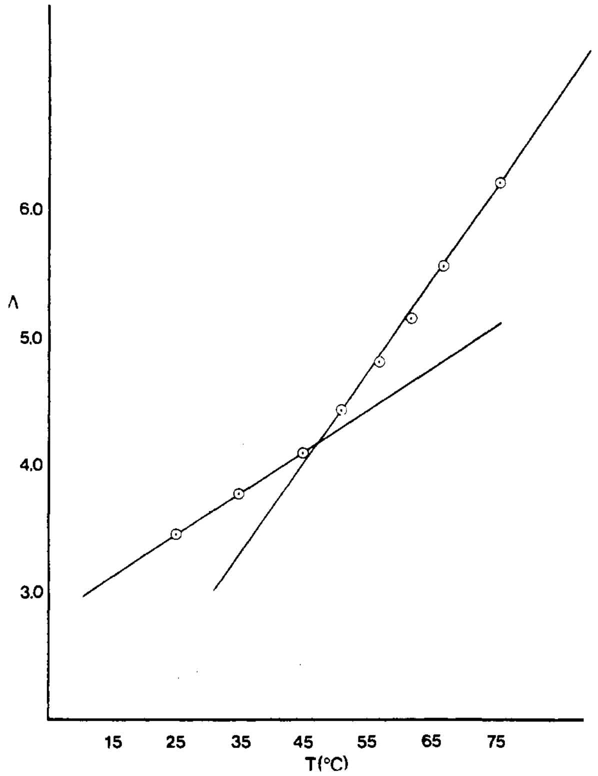

Figure 2. Plot of equivalent conductivity of 0.0107 M VCl_3 in CH_3CN as a function of temperature.

The intensity of the high-temperature peak indicated that it was present in large quantity.

Et_4NBr is known to be a completely dissociated 1:1 electrolyte in CH_3CN. Consequently, any changes in its equivalent conductivity with temperature cannot be due to change in degree of dissociation. The temperature dependence of the equivalent conductivity of 1.048×10^{-3} M Et_4NBr in CH_3CN was determined. The values are found in Table II.

A least-squares plot of this data in eq 1 yields a value of 0.00845 for x for CH_3CN.

The equivalent conductivity, Λ, of a solution of 0.0107 M VCl_3 in CH_3CN was measured as a function of temperature. The results are given in Table III.

A plot of this data is shown in Figure 2. The break in the slope shows the presence of the expected second species. The values

---

(8) Fried, V.; Hameka, H. F.; Blukis, U. *Physical Chemistry*; MacMillan: New York, 1977; p 867.

(9) Nakamoto, K. *Infrared Spectra of Inorganic and Coordination Compounds*, 2nd ed.; Wiley-Interscience: New York, 1970; p 114.

of Λ(calcd) in Table III were obtained by using eq 1 with $x = 0.008\,45$ and $\Lambda_{25} = 3.46$ cm^2 mol^{-1} Ω^{-1}. The difference between Λ and Λ(calcd) in Table III is due to the existence of the second species.

Discussion

The temperature dependence of the ^{1}H NMR line width shows that, as in the case of $TiCl_3$–CH_3CN, two species exist in solutions of VCl_3 in CH_3CN. The temperature dependence of the equivalent conductivity lends support to this idea. The low values of the equivalent conductivity at all temperatures show that not much ionization occurs. Thus, the two species present must be *fac*- and *mer*-$VCl_3 \cdot 3CH_3CN$. It has been established by ESR measurements that at low temperatures the *fac* isomer is present in the $TiCl_3$–CH_3CN system.[7,10] It is likely that the same holds for VCl_3 in CH_3CN. It the amount of the *mer* isomer increases, the conductivity should increase slightly since this isomer and its ions are expected to be more mobile than the more polar *fac* species.[11] This is in agreement with the shape of the curve shown in Figure 2.

---

(10) Giggenbach, W.; Brubaker, C. H., Jr. *Inorg. Chem.* **1969**, *8*, 1131.

(11) Carassiti, V. *Gazz. Chim. Ital.* **1954**, *84*, 405.

Contribution from the Department of Chemistry,
Northeastern University, Boston, Massachusetts 02115

Stoichiometry and Kinetics of the Low-Temperature Oxidation of $L_2Cu_2Cl_2$ (L = *N,N,N',N'*-Tetraethylethylenediamine) by Dioxygen in Methylene Chloride and Properties of the Peroxocopper Products

Geoffrey Davies,* Mohamed A. El-Sayed,*† and Maher Henary

Received October 21, 1986

The dimeric copper(I) complex LCu(Cl,Cl)CuL (D; L is *N,N,N',N'*-tetraethylethylenediamine) completely reduces dioxygen at ambient temperatures in aprotic solvents to give the green, dimeric oxocopper(II) complex LCu(Cl,O,Cl)CuL (C). This study shows that C is the primary oxidation product at temperatures above −26 °C but that two forms of a blue, tetranuclear, mixed-valence peroxocopper complex, A and B, exist in equilibrium at lower temperatures. The blue products were characterized by electronic, ESR, and Raman spectroscopy and by kinetic measurements. Observations that the rate of conversion of A and B to C is critically dependent on temperature in the range ca. −40 to ca. −30 °C are explained by assigning $\Delta H_{11}^{*} = 25 \pm 0.5$ kcal mol^{-1} and $\Delta S_{11}^{*} = 40 \pm 3$ cal deg^{-1} mol^{-1} to this process. Copper complexes A, B, and C initiate the oxidative coupling of 2,6-dimethylphenol by dioxygen. Studies of the catalytic oxidation of excess phenol at −45, −25, and 0 °C show that the proportion of the diphenoquinone product increases very sharply at −45 °C, strongly suggesting that a catalytic cycle involving D/A,B species is responsible for this change of product distribution.

Introduction

Catalysis of dioxygen reactions by the copper(I)–copper(II) couple requires at least partial dioxygen reduction by copper(I).[1-7] Recent reviews[5,6] demonstrate substantial progress in understanding aprotic copper(I)–dioxygen chemistry in the absence of substrates. The primary stoichiometries with oxidation-resistant[6,7] ligands on copper are eq 1–5 (ligands omitted), where Cu^{I}, Cu^{I}_{2}

$$2[Cu^{I}]^{+} + O_2 \rightleftarrows [Cu^{II}O_2Cu^{II}]^{2+} \qquad (1)$$

$$[Cu^{I}_{2}]^{2+} + O_2 \rightleftarrows [Cu^{II}O_2Cu^{II}]^{2+} \qquad (2)$$

$$4Cu^{I} + O_2 \rightarrow Cu^{II}_{4}O_2 \qquad (3)$$

$$2Cu^{I}_{2} + O_2 \rightarrow Cu^{II}_{4}O_2 \qquad (4)$$

$$2Cu^{I}_{2} + O_2 \rightarrow 2Cu^{II}_{2}O \qquad (5)$$

and Cu^{I}_{4} represent copper(I) monomers, dimers, and tetramers, respectively.

Equation 1 was observed by Wilson et al. at ambient temperatures.[8] Particular ligand systems create cationic dioxygen carriers with respectable repeat cycling reproducibility.[8] Karlin et al.[5,9-11] have designed copper(I) dimers containing two N_3Cu^{+} centers that also reversibly bind dioxygen, eq 2, but only at low temperatures. Thompson[12] has even isolated blue, solid $[(TEED)Cu(O_2,H_2O)Cu(TEED)](ClO_4)_2$ (TEED is *N,N,N',N'*-tetraethylethylenediamine), which has an absorption maximum at 630 nm and shows clear evidence for bound peroxide in its ir spectrum.

The copper systems in all of this work[4,8-12] have copper–copper distances that are large enough to accommodate μ(1,2)-peroxo bridges, as also appears to be the case in oxyhemocyanins and oxytyrosinases.[4,5]

The positive charges on the species in eq 1 and 2 probably inhibit reduction by $[Cu^{I}]^{+}$ and $[Cu^{I}_{2}]^{2+}$, respectively (eq 6). Steric bulk

$$[Cu^{II}O_2Cu^{II}]^{2+} + [Cu^{I}_{2}]^{2+} \rightarrow 2[Cu^{II}_{2}O]^{2+} \qquad (6)$$

---

† On leave of absence from the Department of Chemistry, Faculty of Science, Alexandria University, Alexandria, Egypt.

(1) For an excellent collection of papers on many important aspects of copper chemistry see: *Biological and Inorganic Copper Chemistry*; Karlin, K. D., Zubieta, J., Eds.; Adenine: Guilderland, NY, **1986**; Vol. 1 and 2.

(2) Davies, G.; El-Sayed, M. A. In *Copper Coordination Chemistry: Biochemical and Inorganic Perspectives*; Karlin, K. D., Zubieta, J. A., Eds.; Adenine: Guilderland, NY, **1983**, p 281.

(3) Speier, G.; Tyeklár, Z. In *Biological and Inorganic Copper Chemistry*; Karlin, K. D.; Zubieta, J., Eds.; Adenine: Guilderland, NY, 1986; Vol. 2, p 91.

(4) Wilcox, D. E.; Porras, A. G.; Hwang, Y. T.; Lerch, K.; Winkler, M. E.; Solomon, E. I. *J. Am. Chem. Soc.* **1985**, *107*, 4015 and references therein.

(5) Karlin, K. D.; Gultneh, Y. *J. Chem. Educ.* **1985**, *62*, 983 and references therein; Karlin, K. D.; Gultneh, Y. *Prog. Inorg. Chem.*, in press.

(6) Davies, G.; El-Sayed, M. A. *Comments Inorg. Chem.* **1985**, *4*, 151.

(7) Davies, G.; El-Shazly, M. F.; Kozlowski, D. R.; Kramer, C. E.; Rupich, M. W.; Slaven, R. W. *Adv. Chem. Ser.* **1979**, *No. 173*, 178.

(8) Goodwin, J. A.; Stanbury, D. M.; Wilson, L. J. in *Biological and Inorganic Copper Chemistry*; Karlin, K. D.; Zubieta, J., Eds.; Adenine: Guilderland, NY, 1986; Vol. 2, p 11 and references therein.

(9) Karlin, K. D.; Cruse, R. W.; Gultneh, Y.; Hayes, J. C.; Zubieta, J. *J. Am. Chem. Soc.* **1984**, *106*, 3372.

(10) Karlin, K. D.; Cruse, R. W.; Gultneh, Y.; Hayes, J. C.; McKown, J. W.; Zubieta, J. In *Biological and Inorganic Copper Chemistry*; Karlin, K. D.; Zubieta, J., Eds.; Adenine: Guilderland, NY, 1986; Vol. 2, p 101.

(11) Karlin, K. D.; Haka, M. S.; Cruse, R. W.; Gultneh, Y. *J. Am. Chem. Soc.* **1985**, *107*, 5828.

(12) Thompson, J. S. In *Biological and Inorganic Copper Chemistry*; Karlin, K. D.; Zubieta, J., Eds.; Adenine: Guilderland, NY, 1986; Vol. 2, p 1 and references therein.

0020-1669/87/1326-3266$01.50/0